DOI: 10.1002/ange.201206227

Luminescent Motion

Light-Emitting Electrochemical "Swimmers"**

Milica Sentic, Gabriel Loget, Dragan Manojlovic, Alexander Kuhn, and Neso Sojic*

Controlling the motion of small objects is of crucial importance for many potential applications ranging from micromotors to nanomedicine and has generated huge interest in the scientific community in recent years. In this context, tracking such moving objects in real time is a challenge and therefore tremendous effort has been made to design particles with specific optical, in many cases fluorescent, properties. Herein, we propose an original approach, where an object is simultaneously moving and emitting light, produced by electrogenerated chemiluminescence. This phenomenon is based on the concept of bipolar electrochemistry, which is not only the driving force for the propulsion of the particle, but also for the emission of light, combining two redox reactions on one object.

Biomotors are a great source of inspiration for chemists.[1] Within this context, an important and multidisciplinary area of research is devoted to the construction and study of micro- and nanomotors.[2] Designing such objects, which can mimic the propulsion of biological systems in artificial and biological environments has moved to the forefront of science over the last decade.[3] The spontaneous hydrolysis of adenosine triphosphate (ATP), which supplies biomolecular motors with energy in natural systems, has been mimicked in most of the strategies developed to generate motion with micro-objects.[4] The concept is based on the use of a chemical fuel to generate self-electrophoresis or bubble propulsion.[4,5]

Although this approach has been widely used, because of its convenience and the attainable speed, it also has a few disadvantages, such as the use of such fuels[5a,6] may not be compatible with some media. Therefore, alternative approaches based on external stimuli are highly important.[7] The use of magnetic fields has been explored and already provided some applications for cargo towing at the microscale.[14,15] Other fuel-free methods based on electric fields, either direct or alternating current, have been developed for manipulating propellers.[8] In this context, mechanisms such as electrophoresis, dielectrophoresis, and induced-charged electrophoresis have been explored to generate particle motion.[9] In a complementary approach used herein, electrochemical reactions can be induced when polarizing a conducting object in an electric field. This wireless concept, also called bipolar electrochemistry, is based on the fact that when a conducting particle is placed in an electric field, a polarization voltage occurs between both extremities of the particle.[10] This polarization is proportional to the electric field and to the dimensions of the object. If the polarization voltage is high enough, redox reactions can be carried out at the opposite sides of the particle, oxidation reactions at the anodic pole are simultaneous with reduction reactions at the cathodic pole. The spatial selectivity that this phenomenon provides has been recently applied to analytical chemistry,[10b,11] materials science,[12] and also to propel "swimmers".[13] Advantages of this technique are the motion control provided by the field strength/direction and its versatility, because any kind of conducting object can theoretically act as a swimmer.

The observation of such swimmers is generally a challenge and usually requires an efficient microscopy set up[5a] or swimmers tagged with fluorescent molecules[14] to monitor their motion. In this context, it would be helpful if the swimmer could also act as an autonomous light source, with the photon emission being intrinsically coupled to the motion. Light can be emitted by a number of luminescent processes, including electrogenerated chemiluminescence (ECL). ECL is a widely used electrochemical process that has the advantage of not requiring an excitation light source.[15] Indeed, ECL is the light emitted by the excited state of a luminophore, resulting from an initial electron transfer reaction occurring at the electrode surface. ECL is a powerful and extremely sensitive detection method, which has been reported for a number of assays.[16] The majority of ECL applications reported so far involve $[Ru(bpy)_3]^{2+}$ (bpy = 2,2′-bipyridine) or its derivatives as the light-emitting species and tri-*n*-propylamine (TPrA) as the co-reactant, because the $[Ru(bpy)_3]^{2+}$/TPrA system exhibits high ECL efficiency. Therefore, this model system forms the basis of commercially available ECL immunoassays.[15b] The combination of ECL and bipolar electrochemistry has already been used for analytical purposes.[10b] Manz and co-workers used ECL generation at the anodic pole of a bipolar electrode for the detection of amines[17] and Crooks and co-workers have pioneered its use for many other analytical purposes.[18] Herein, we use ECL for the coupling of light emission and gas bubble production, to propel light-emitting bipolar electrochemical swimmers.

As recently reported, translation, rotation, and levitation of conducting particles can be triggered by bipolar electro-

---

[*] M. Sentic, G. Loget, Prof. A. Kuhn, Prof. N. Sojic
Institut des Sciences Moléculaires, CNRS UMR 5255
University of Bordeaux, ENSCBP
33607 Pessac (France)
E-mail: soji@enscbp.fr
Homepage: http://www.enscbp.fr/nsysa/home.asp
M. Sentic, Prof. D. Manojlovic
Faculty of Chemistry, University of Belgrade
11000 Belgrade (Serbia)

[**] We acknowledge financial support from the Ministry of Science and Technological Development (Republic of Serbia) and from the French Foreign Ministry (Programme Pavle Savic). Further financial support has been received from CNRS and the Agence Nationale de la Recherche (ANR-09-BLAN-0418; ANR-08-NSCI-008-01).

Supporting information for this article (experimental details) is available on the WWW under http://dx.doi.org/10.1002/anie.201206227.

chemistry.[13] Among the reported mechanisms, the most versatile involves the reduction of water [Eq. (1)]:

$$H_2O_{(l)} + e^- \rightarrow {}^1\!/_2 H_{2(g)} + OH^-_{(l)} \qquad (1)$$

at the cathodic pole of the bipolar swimmer.[13b,c] This reaction induces the asymmetric generation and release of H_2 bubbles, which create local hydrodynamic forces at the bipolar electrode (BE) surface. As a consequence, motion is generated in the direction opposite of the bubble release. Because of charge neutrality during bipolar electrochemistry, water or a sacrificial molecule such as hydroquinone must be oxidized simultaneously at the anodic pole, generating oxidation products such as O_2 or benzoquinone.[13a,b] These anodic reactions are not useful in the context of propulsion and can therefore be replaced by electrochemical reactions, leading to ECL emission.

The ECL mechanism of the reaction of TPrA with $[Ru(bpy)_3]^{2+}$ is an active area of investigation[19] and it depends on several experimental parameters (for example, surface hydrophobicity, electrode material, concentration ratio, pH value, and presence of surfactant).[20] In brief, the mechanism involves oxidation of both species, which then react together to produce the excited state of the $[Ru(bpy)_3]^{2+}$ luminophore and thus, ECL emission.[19] As depicted in Figure 1, the asymmetric electroactivity induced by bipolar electrochemistry generates simultaneous motion and light emission of a bipolar swimmer. Indeed, these effects result from the cooperative reduction of H_2O at the cathodic pole and oxidation of the ECL reagents at the anodic pole of the bead.

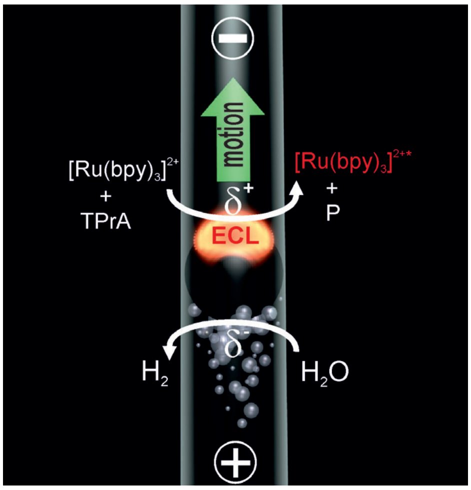

Figure 1. Asymmetric light-emitting electrochemical swimmer. Simultaneous reduction of H_2O at the cathodic pole (bottom of the bead) and oxidation of ECL reagents at the anodic pole (top of the bead) induces both motion and light emission from the bead in a glass capillary. P corresponds to a side product of the TPrA radicals formed during the ECL process.

A difference in potential between the poles of the object is required to simultaneously generate the gas bubbles and ECL, so to estimate this difference the corresponding redox reactions have been characterized by cyclic voltammetry with a normal working electrode composed of the swimmer material (see Supporting Information for experimental details). This electrochemical measurement has been combined with a simultaneous monitoring of the ECL intensity. Typical voltammetric and ECL responses are presented in the Supporting Information, Figure S2. From these curves, the potential values for which the different redox reactions are occurring at the swimmer surface can be easily calculated. Water reduction (Equation 1) takes place at $E_{red} = -1.1$ V versus Ag/AgCl and ECL emission occurs at $E_{ox} = 1$ V versus Ag/AgCl.

The polarization voltage ΔV induced on a conducting object is proportional to the external electric field E and the diameter of the bead l,[11b] as described by the simple relation [Eq. (2)]:

$$\Delta V = E\,l \qquad (2)$$

Based on the experimentally determined values of E_{red} and E_{ox}, one can conclude that the coupling of water reduction and ECL emission at the reactive poles of a BE is possible only if the polarization potential ΔV between both extremities of the BE is at least equal to $|E_{red} - E_{ox}| = 2.1$ V. Equation (2) thus states that for a BE having a diameter l of about 1 mm, the electric field E has to be, in a first-order approximation, at least 21 $V\,cm^{-1}$.

Levitation experiments were achieved in a U-shaped glass cell (Figure S1).[13c] Glassy carbon (GC) was chosen as the swimmer material because of its low density compared to many other conducting materials, such as metals. This low density decreases the force needed to overcome gravity for an object with a given volume. The cell was maintained in a vertical position and the GC bead was inserted into one arm of the cell. Because of the slightly conical shape of the capillary tube, the bead dropped until it was stopped by the capillary walls. The feeder electrodes were inserted into the top part of the cell and were polarized in such a way that the H_2 bubbles were generated underneath the bead, as illustrated in Figure 1. The distance between both electrodes was 9.8 cm and the applied voltage was 250 V, this corresponded to a global electric field of $E = 25.5\ V\,cm^{-1}$. This value is above the previously calculated theoretical threshold value of 21 $V\,cm^{-1}$ and therefore, leads to the simultaneous levitation/ECL emission of the GC bead under these conditions, as demonstrated by Video S1 and Figure 2.

The left picture of Figure 2, obtained under ambient light, shows the GC bead in the capillary. The bead is spherical, but appears slightly stretched along its equatorial axis owing to an optical effect of the cylindrical capillary. As shown in Video S1 and Figure 2, the light was then turned off and an electric field applied. The ECL generated at the anodic pole of the BE was extremely bright and it could be instantaneously observed with the naked eye or with a mobile phone camera.[21] The ECL images presented in Figure 2 were recorded with a consumer digital camera. The initial time $t = 0$ s was defined as the time when the camera became focused on the ECL signal. After six seconds, levitation began owing to H_2 bubble production below the bead;[13c] a phenomenon that could be clearly observed when the ambient light

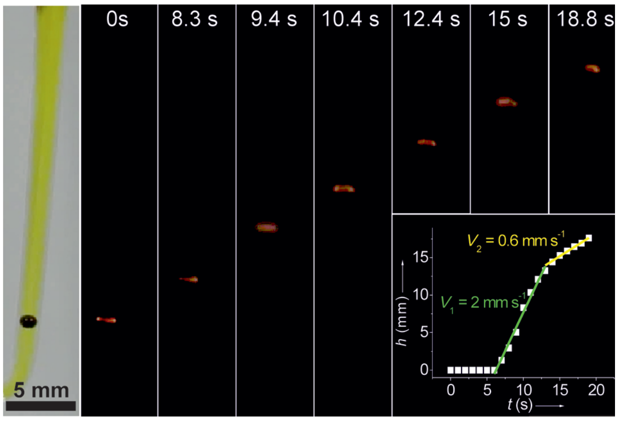

Figure 2. Levitation of a light-emitting GC bead. Series of optical images showing a GC bead emitting ECL at different times during its motion. The bead was placed in a U-shaped cell, filled with 100 mM PBS buffer containing 0.5 mM $[Ru(bpy)_3]^{2+}$, 100 mM TPrA, and a few drops of surfactant. It was exposed to an external electric field of $25.5\ \text{V cm}^{-1}$. The left image was taken under white light and the other images were taken in the dark. Inset: Plot showing the change in height h of the bead as a function of time t.

was turned on during the bead motion. A surfactant was added to the solution to promote the formation of homogeneous H_2 bubbles and facilitate their continuous release from the bead surface, resulting in a more regular motion.[13c]

The inset of Figure 2 shows the height of the ECL bead as a function of time. Height h was defined as the distance between the equatorial axis of the immobilized bead on the left picture and the center of the ECL emitting area during the motion. This curve can be divided into three distinct parts, from which the speed can be extracted based on the slope. In the first part of the curve, the bead did not move. This part corresponds to the period of bubble accumulation underneath the bead for the generation of a sufficiently high buoyancy to overcome gravity. After this initial phase, the change in height was linear for seven seconds at a speed $v_1 = 2\ \text{mm s}^{-1}$ or approximately two bead-lengths per second. Finally, because the shape of the cell arm is slightly conical (see left picture of Figure 2), the space between the bead and the glass walls became larger as the bead rose, thus allowing the bubbles to escape from below the bead, which lead to a decrease of the speed during the third phase ($v_1 = 0.6\ \text{mm s}^{-1}$). The levitation was stopped by switching off the electric field. This caused the bead to drop and a new rise could be triggered by reapplying the electric field. The height and speed of levitation is comparable to the ones reported without ECL,[13c] showing that the ECL mechanism does not affect the bead propulsion. According to Figure 1, the ECL profile should follow the shape of the anodic pole, leading to a lightened hemisphere at the top of the bead. This was the case at certain moments of the experiment, but during the run a more ring-like ECL shape was also observed. To understand these changes, we further investigated the parameters affecting the ECL profile at the GC beads.

The pH value is a crucial parameter in the ECL process of the model TPrA/$[Ru(bpy)_3]^{2+}$ system. ECL is known to occur at pH values greater than 5.5, with a maximum ECL intensity at pH 7.5. TPrA is insoluble at higher pH values and is protonated at lower pH values, which greatly inhibits the ECL emission.[22] This is the reason we used PBS buffer in these experiments, ensuring a constant pH value of 7.4 under normal conditions. But, depending on the applied potential, water may also be oxidized at the anodic hemisphere of the bead following the reaction [Eq. (3)]:

$$H_2O_{(l)} \rightarrow {}^{1}\!/_{2}\, O_{2(g)} + 2\,H^{+}{}_{(l)} + 2\,e^{-} \qquad (3)$$

The beginning of the oxidation wave corresponding to this reaction can be observed in Figure S2. It starts at a more anodic potential than the ECL reactions, around 1.5 V versus Ag/AgCl. The theoretical polarization voltage required to achieve simultaneous water reduction (Equation 1) at the cathodic pole and ECL emission and water oxidation (Equation 3) at the anodic pole corresponds to $|-1.1-1.5| = 2.6\ \text{V}$. This value fits with the value of ΔV applied in Figure 2. This suggests that water oxidation may occur at the very top of the bead where the polarization potential is the highest. Therefore, it would induce a local pH decrease.

To check the variation in pH value, experiments were performed in the presence of a pH indicator. A GC bead was exposed to the same electric field as before. The medium was also identical except that no surfactant was present and a few drops of a universal pH indicator were added to the solution. Figure 3b shows clearly that pH variations occur at the reactive poles of the BE during these experiments. Indeed,

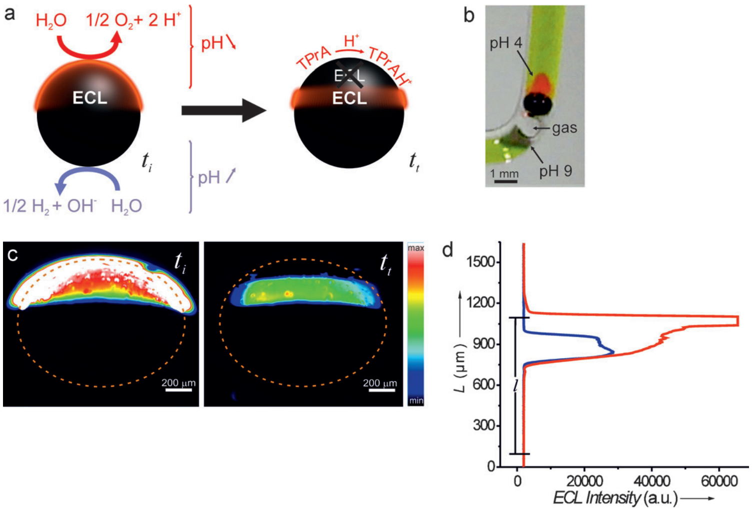

Figure 3. a) Mechanism responsible for the shape of the ECL-emitting regions on the bead. b) Optical micrograph of a GC bead in the U-shaped cell filled with 100 mM PBS, 0.5 mM $[Ru(bpy)_3]^{2+}$, 100 mM TPrA, and a universal pH indicator with a $25.5\ \text{V cm}^{-1}$ external electric field. c) Images showing the evolution of the ECL shapes on a GC bead in a U-shaped cell filled with 100 mM PBS, 0.5 mM $[Ru(bpy)_3]^{2+}$, and 100 mM TPrA at $t = t_i$ (left) and $t = t_t$ (right). A potential of 75 V was applied between the feeder electrodes. Dashed lines show the position of the GC bead. d) ECL intensity profiles from (c) taken along the middle vertical axis of the bead at t_i (red) and t_t (blue). l = bead diameter.

water reduction, which produces the H_2 gas bubble, also induces an increase in pH (Equation 1) up to a value of approximately pH 9. The absence of surfactant caused the H_2 accumulation, producing the large bubble that can be seen at the bottom of the bead. At the top of the bead, the pH reaches a value of 4, confirming that water oxidation also takes place at the anodic pole. This experiment confirmed that ECL reactions are in competition with water oxidation at the anodic pole of the bead. This reaction directly influences the ECL process because it induces a local pH decrease, leading to TPrA protonation, which causes a loss of ECL at the top part of the bead, thus creating an ECL ring instead of a hemispherical shape (Figure 3 a).

We further investigated the influence of parameters such as applied voltage and buffer capacity, which directly affect the pH gradient around the bead and thus the ECL profile (Figure 3 c; Figures S3, S4). A voltage of 75 V was applied at the feeder electrodes and initially generated a hemispherical ECL shape (Figure 3 c). The ECL was limited to the anodic part of the bead and no ECL was detected at the cathodic pole. The ECL-emitting region did not expand into the solution surrounding the bead, but was confined to the bead surface by the high TPrA concentration, which limits the thickness of the electrocatalytic ECL reaction layer.[23] The hemisphere observed at t_i changes rapidly to a transient state at t_t, typically after a few seconds (Figure 3 c). The ECL intensity was drastically suppressed in the upper part of the previously ECL-emitting region at time t_t, whereas it remained constant for the equatorial region (Figure 3 d). Such behavior can be rationalized by the mechanism illustrated in Figure 3 a. At 75 V, protons were formed at the anodic pole of the bead. At the initial stage t_i, the buffer capacity is strong enough to avoid TPrA protonation, thus the ECL-emitting region is not affected. The electrogenerated pH gradients were progressively established at the anodic pole of the bead and the local pH variation limited the ECL region to a ring shape after a few seconds (t_t). These experiments demonstrate that the ECL shape can be fine-tuned using easily controllable parameters such as the electric field or the buffer concentration.

In this work, we presented the synergetic action of bipolar electrochemistry in terms of simultaneous bubble production and ECL generation, leading to the first example of a propulsion mechanism for a swimmer that is coupled with a chemical light source. The shape of the ECL undergoes an interesting evolution during the run, and we demonstrated that this is related to a pH decrease at the anodic pole of the swimmer. Herein, we have shown that motion on the macroscopic scale occurs concomitantly with light emission. ECL provided a method for directly monitoring of the motion of the object, which is very useful in the context of autonomous swimmers. The versatility of bipolar electrochemistry coupled to ECL could allow the same principle to be applied to other types of swimmers and at smaller scales. It therefore opens the door to a new class of dynamic experiments with multifunctional objects. For instance, dynamic multiplexed immunoassays or DNA assays could be developed in solution phase with biofunctionalized swimmers, using ECL as a readout. Finally, such an ECL swimmer resembles biological systems, and the present system could be considered an artificial analogue of bioluminescent fish or other light-emitting marine creatures.

Received: August 3, 2012

Keywords: chemiluminescence · electrochemistry · redox chemistry · swimmers

---

[1] a) M. Schliwa, G. Woehlke, *Nature* **2003**, *422*, 759 – 765; b) A. Goel, V. Vogel, *Nat. Nanotechnol.* **2008**, *3*, 465 – 475; c) T. Fischer, A. Agarwal, H. Hess, *Nat. Nanotechnol.* **2009**, *4*, 162 – 166; d) M. G. L. van den Heuvel, C. Dekker, *Science* **2007**, *317*, 333 – 336; e) S. J. Ebbens, J. R. Howse, *Soft Matter* **2010**, *6*, 726 – 738.

[2] a) W. F. Paxton, S. Sundararajan, T. E. Mallouk, A. Sen, *Angew. Chem.* **2006**, *118*, 5546 – 5556; *Angew. Chem. Int. Ed.* **2006**, *45*, 5420 – 5429; b) Y. Mei, A. A. Solovev, S. Sanchez, O. G. Schmidt, *Chem. Soc. Rev.* **2011**, *40*, 2109 – 2119.

[3] a) R. F. Ismagilov, A. Schwartz, N. Bowden, G. M. Whitesides, *Angew. Chem.* **2002**, *114*, 674 – 676; *Angew. Chem. Int. Ed.* **2002**, *41*, 652 – 676; b) R. Dreyfus, J. Baudry, M. L. Roper, M. Fermigier, H. A. Stone, J. Bibette, *Nature* **2005**, *437*, 862 – 865; c) Y. Wang, R. M. Hernandez, D. J. Bartlett, J. M. Bingham, T. R. Kline, A. Sen, T. E. Mallouk, *Langmuir* **2006**, *22*, 10451 – 10456; d) K. M. Manesh, M. Cardona, R. Yuan, M. Clark, D. Kagan, S. Balasubramanian, J. Wang, *ACS Nano* **2010**, *4*, 1799 – 1804.

[4] D. A. Wilson, R. J. M. Nolte, J. C. M. van Hest, *Nat. Chem.* **2012**, *4*, 268 – 274.

[5] a) R. Laocharoensuk, J. Burdick, J. Wang, *ACS Nano* **2008**, *2*, 1069 – 1075; b) A. A. Solovev, W. Xi, D. H. Gracias, S. M. Harazim, C. Deneke, S. Sanchez, O. G. Schmidt, *ACS Nano* **2012**, *6*, 1751 – 1756; c) W. Gao, A. Pei, J. Wang, *ACS Nano* **2012**, *6*, 8432 – 8438.

[6] W. Gao, A. Uygun, J. Wang, *J. Am. Chem. Soc.* **2012**, *134*, 897 – 900.

[7] a) S. Tottori, L. Zhang, F. Qiu, K. K. Krawczyk, A. Franco-Obregón, B. J. Nelson, *Adv. Mater.* **2012**, *24*, 811 – 816; b) W. Gao, S. Sattayasamitsathit, K. M. Manesh, D. Weihs, J. Wang, *J. Am. Chem. Soc.* **2010**, *132*, 14403 – 14405.

[8] O. D. Velev, S. Gangwal, D. N. Petsev, *Annu. Rep. Sec. C* **2009**, *105*, 213 – 246.

[9] a) S. T. Chang, V. N. Paunov, D. N. Petsev, O. D. Velev, *Nat. Mater.* **2007**, *6*, 235 – 240; b) S. Gangwal, O. J. Cayre, M. Z. Bazant, O. D. Velev, *Phys. Rev. Lett.* **2008**, *100*, 058302; c) C. Zhang, K. Khoshmanesh, A. Mitchell, K. Kalantar-zadeh, *Anal. Bioanal. Chem.* **2009**, *396*, 401 – 420.

[10] a) M. Fleischmann, J. Ghoroghchian, D. Rolison, S. Pons, *J. Phys. Chem.* **1986**, *90*, 6392 – 6400; b) F. Mavré, R. K. Anand, D. R. Laws, K.-F. Chow, B.-Y. Chang, J. A. Crooks, R. M. Crooks, *Anal. Chem.* **2010**, *82*, 8766 – 8774.

[11] a) S. E. Fosdick, R. M. Crooks, *J. Am. Chem. Soc.* **2012**, *134*, 863 – 866; b) G. Loget, A. Kuhn, *Anal. Bioanal. Chem.* **2011**, *400*, 1691 – 1704.

[12] a) Y. Ishiguro, S. Inagi, T. Fuchigami, *Langmuir* **2011**, *27*, 7158 – 7162; b) R. Ramaswamy, C. Shannon, *Langmuir* **2011**, *27*, 878 – 881; c) G. Loget, V. Lapeyre, P. Garrigue, C. Warakulwit, J. Limtrakul, M.-H. Delville, A. Kuhn, *Chem. Mater.* **2011**, *23*, 2595 – 2599.

[13] a) G. Loget, A. Kuhn, *J. Am. Chem. Soc.* **2010**, *132*, 15918 – 15919; b) G. Loget, A. Kuhn, *Nat. Commun.* **2011**, *2*, 535; c) G. Loget, A. Kuhn, *Lab Chip* **2012**, *12*, 1967 – 1971.

[14] a) A. Ghosh, P. Fischer, *Nano Lett.* **2009**, *9*, 2243–2245; b) S. J. Ebbens, J. R. Howse, *Langmuir* **2011**, *27*, 12293–12296.

[15] a) A. J. Bard, *Electrogenerated Chemiluminescence*, Maceler Dekker Inc, New York, **2004**; b) W. Miao, *Chem. Rev.* **2008**, *108*, 2506–2553.

[16] a) N. Sardesai, S. Pan, J. Rusling, *Chem. Commun.* **2009**, 4968–4970; b) F. Deiss, C. N. LaFratta, M. Symer, T. M. Blicharz, N. Sojic, D. R. Walt, *J. Am. Chem. Soc.* **2009**, *131*, 6088–6089; c) W. Miao, A. J. Bard, *Anal. Chem.* **2004**, *76*, 7109–7113.

[17] A. Arora, J. C. T. Eijkel, W. E. Morf, A. Manz, *Anal. Chem.* **2001**, *73*, 3282–3288.

[18] a) W. Zhan, J. Alvarez, R. M. Crooks, *Anal. Chem.* **2003**, *75*, 313–318; b) K.-F. Chow, F. Mavré, R. M. Crooks, *J. Am. Chem. Soc.* **2008**, *130*, 7544–7545; c) K.-F. Chow, F. Mavré, J. A. Crooks, B.-Y. Chang, R. M. Crooks, *J. Am. Chem. Soc.* **2009**, *131*, 8364–8365.

[19] a) W. Miao, J.-P. Choi, A. J. Bard, *J. Am. Chem. Soc.* **2002**, *124*, 14478–14485; b) F. Kanoufi, Y. Zu, A. J. Bard, *J. Phys. Chem. B* **2000**, *105*, 210–216.

[20] a) Y. Zu, A. J. Bard, *Anal. Chem.* **2001**, *73*, 3960–3964; b) S. Workman, M. M. Richter, *Anal. Chem.* **2000**, *72*, 5556–5561.

[21] J. L. Delaney, C. F. Hogan, J. Tian, W. Shen, *Anal. Chem.* **2011**, *83*, 1300–1306.

[22] a) K. L. Jonathan, J. P. Michael, *J. Electrochem. Soc.* **1990**, *137*, 3127–3131; b) A. W. Knight, G. M. Greenway, *Analyst* **1996**, *121*, 101R–106R; c) D. Badocco, F. Zanon, P. Pastore, *Electrochim. Acta* **2006**, *51*, 6442–6450.

[23] Y. Zu, Z. Ding, J. Zhou, Y. Lee, A. J. Bard, *Anal. Chem.* **2001**, *73*, 2153–2156.